HHS Public Access

Author manuscript

Electrophoresis. Author manuscript; available in PMC 2018 March 01.

Published in final edited form as:

Electrophoresis. 2017 March ; 38(5): 738–746. doi:10.1002/elps.201600381.

Phospholipid bilayer affinities and solvation characteristics by electrokinetic chromatography with a nanodisc pseudostationary phase

William M. Penny, **Harmen B. Steele**, **J.B. Alexander Ross**, and **Chistopher P. Palmer**

Department of Chemistry and Biochemistry, University of Montana, Missoula, MT 59803 USA

Abstract

Phospholipid bilayer nanodiscs composed of 1,2-dimyristoyl-*sn*-glycero-3-phosphocholine and synthetic maleic acid-styrene copolymer belts have been introduced as a pseudostationary phase (PSP) in electrokinetic chromatography and demonstrated good performance. The nanodiscs provide a suitable migration range and high theoretical plate counts. Using this nanodisc PSP, the affinity of the bilayer structure for probe solutes was determined and characterized. Good correlation is observed between retention factors and octanol water partition coefficients for particular categories of solutes, but the general correlation is weak primarily because the nanodiscs show stronger affinity than octanol for hydrogen bond donors. This suggests that a more appropriate application of this technology is to measure and characterize interactions between solutes and lipid bilayers directly. Linear solvation energy relationship analysis of the nanodisc-solute interactions in this study demonstrates that the nanodiscs provide a solvation environment with low cohesivity and weak hydrogen bond donating ability, and provide relatively strong hydrogen bond acceptor strength.

Keywords

electrokinetic chromatography; phospholipid bilayer; nanodisc; linear solvation energy relationships; DMPC

1. Introduction

Electrokinetic Chromatography (EKC) is a variation of capillary electrophoresis developed in 1984 by Terabe et al.[1] In this form of chromatography, analytes are separated via selective interactions with a pseudostationary phase (PSP) dispersed within the CE background electrolyte (BGE). The theory, applications and development of the technique have been presented in textbooks and reviews.[2, 3] The first PSPs were surfactant micelles, but since that time several different types of PSPs have been introduced in attempts to offer different separation selectivity or to improve performance. Microemulsions[4, 5], polymers[6–8] nanoparticles[9, 10], liposomes[11, 12] and vesicles[12, 13] are just a few of

The authors have declared no conflicts of interest.

the forms that have been described in the literature. This technology allows for fast, selective, and efficient separations that require only nanoliter sample volumes.

The utility of EKC to characterize PSPs and PSP–solute interactions has been recognized since its introduction[1]. A major application of EKC has been to measure the affinity between solutes and a PSP as a proxy for affinity for biological lipid bilayers or for octanol-water partition coefficients ($P_{o/w}$). Measurement of lipophilicity, as described by $P_{O/W}$ or D (measured or calculated under specific conditions), is important in pharmaceutical development because metabolic clearance rate[14] and biotransport properties can be correlated to lipophilicity[15]. $P_{o/w}$ or D is also a useful measure of potential bioaccumulation and ecotoxicity. The measurement of solute portioning is a primary application of EKC with liposome PSPs[16–21], and this approach has also been used to estimate skin permeability[22, 23], blood-brain barrier transport[24], ecotoxicity[25], and drug-induced phospholipidosis risk[26]. $P_{o/w}$ has most often been correlated with retention factors in microemulsion EKC[27–38], although vesicles have also been investigated for this purpose[15]. Xia *et al.*[37, 38] reported methods to obtain improved correlation of microemulsion EKC results with $P_{o/w}$ values, and microemulsion EKC has been investigated for determination of brain tissue partitioning for central nervous system drugs[39].

Nanodiscs are nanometer scale disc-shaped phospholipid bilayer assemblies encircled by two genetically engineered belt or scaffold proteins[40–43] (see Figure 1[43]). The belt proteins interact with the hydrophobic edges of the nanodisc on the inner side and the surrounding aqueous medium on the outer side, serving to stabilize the nanodiscs in aqueous dispersions. The belt proteins are based on human serum apolipoprotein, and can be generated in different lengths to create nanodiscs of different diameters. The phospholipid composition of the nanodiscs can also be varied to mimic specific biological systems. These phospholipid bilayer structures thus have extraordinary and unique potential to simulate biological membranes and could represent useful constructs with which to study membrane affinities by EKC. Unfortunately, it is prohibitively difficult and expensive to generate enough belt protein to produce nanodiscs in sufficient quantity to carry out EKC studies.

More recently, phospholipid bilayer nanodisc structures have been generated using synthetic styrene-maleic acid copolymers to surround and stabilize the discs in place of belt proteins[44]. The structure of this copolymer lipid nanodisc assembly was studied extensively by Jamshad et al.[45]. The copolymer belt, which contains two styrene monomers for every maleic acid, takes the form of a bracelet encircling the lipid membrane with the styrene oriented parallel to the alkyl chains of the lipid[45]. Using this approach, it is now possible to produce nanodiscs inexpensively in sufficient quantity for use in EKC studies. Furthermore, the anionic maleic acid group serves the purpose of imparting negative charge and electrophoretic mobility on the nanodiscs, making them suitable as a PSP.

In this study we evaluate these phospholipid nanodiscs as a representative model of a lipid bilayer to determine bilayer affinities by EKC. Nanodiscs are generated from 1,2-dimyristoyl-*sn*-glycero-3-phosphocholine (DMPC) lipids and the styrene-maleic acid copolymer. DMPC lipids were chosen for this initial study to generate lipid-polymer discs with uniform composition. DMPC is a net nonionic lipid with no carbon double bonds

leading to a bilayer with minimal disorder. The utility of these nanodiscs as EKC PSPs is demonstrated for the first time, and the retention factors of 38 compounds are correlated to their experimental $P_{o/w}$. All of the compounds were analyzed phosphate BGE in the absence of PSP in order to confirm zero electrophoretic mobility. This allowed for the comparison of Log k' values to Log $P_{o/w}$ values and confirmed that the compounds migrate with electroosmotic flow when not associated with the nanodiscs. LSER analysis is conducted to further understand the interactions between small molecules and the lipid bilayer. Analysis of the results indicates that interactions with the phosphocholine head groups contribute significantly to the affinities of solutes for the nanodiscs.

2. Materials and Methods

2.1 Chemicals

Sodium phosphate monobasic monohydrate, sodium phosphate dibasic heptahydrate, potassium hydroxide, and hydrochloric acid were purchased from Sigma-Aldrich (Saint Louis, MO). 1,2-dimyristoyl-*sn*-glycero-3-phosphocholine (DMPC) lipids were purchased from Avanti Polar Lipids (Alabaster, AL). Copolymer, SMA 2000, was a gift from J. Antoinette Killian of Utrecht University. All analytes used for analysis were obtained from either Sigma-Aldrich (Saint Louis, MO) or ACROS Organics (Geel, Belgium).

2.2 Preparation of copolymer SMA 2000

The SMA 2000 copolymer preparation has been described several times in the literature [46, 47]. Briefly, a 5% (w/v) solution of SMA 2000 is suspended in a 1M KOH solution and refluxed for 6 hours. FTIR analysis, monitoring the shift in the carbonyl signal from 1780cm^{-1} to 1560cm^{-1}, confirmed reaction completion. The copolymer was precipitated using 6M HCl to create a 1.1M HCl solution. The precipitate was washed five times with 0.1M HCl. The copolymer was freeze-dried and stored at room temperature.

2.3 Preparation of nanodiscs

Phospholipids dissolved in chloroform were dried in vacuo and rehydrated to 5mM lipid concentration using a 25 mM phosphate pH 7.0 buffer. Ten freeze-thaw cycles were performed on the lipid solution using a dry ice-ethanol bath and a sonicator with a water temperature set 10°C above the DMPC lipid gel-to-liquid crystalline phase transition temperature (T_m), which is 24°C, to form multilamellar vesicles. Vesicles were extruded through a 200-nm polycarbonate filter using an Avanti mini-extruder at least 13 times to create large unilamellar vesicles[46]. Extrusion provides consistency between preparations but is not required, and the nanodiscs will form from multilamellar vesicles as well. After extrusion a 5% (w/v) solution of SMA 2000 polymer in 25 mM phosphate buffer at an adjusted pH of 7.0 was added such that the solution contained a 1:0.85 (w:w) lipid to copolymer ratio. This ratio was determined to provide stable nanodiscs of suitable diameter for EKC studies in separate studies varying the ratio from 0.5:1 to 1:1. The solution was then lightly vortexed for 5 minutes before being left to sit at room temperature for 2 hours to equilibrate and complete nanodisc formation, and placed in the refrigerator for storage.

2.4 Nanodisc characterization

The size and polydispersity of the nanodiscs were obtained by dynamic light scattering at 5mM phospholipid concentration in 25 mM phosphate buffer pH 7.0 with a Malvern Zetasizer Nano ZS. Four syntheses were measured in three separate trials which consisted of 14–15 measurements per trial.

2.5 EKC Characterization

Phosphate buffers, prepared by dissolving sodium phosphate monobasic and sodium phosphate dibasic in 18MΩ nanopure water from an EMD Millipore system (Bedford, MA) and diluting to 25mM concentration, were used as background electrolyte (BGE) for all analytical separations. A 5 mM phospholipid concentration of nanodiscs in BGE was used for all separations. Stock solutions (25mM) of each analyte were prepared in acetone. Analytical samples were prepared from stock solutions by dilution to 250μm in BGE so that the injected samples contained only 1% acetone. EKC experiments were performed on an Agilent^{3D}CE instrument with on-column DAD controlled by Agilent Chemstation software using 50μm id fused silica capillaries with 150μm extended pathlength cell (Agilent Technologies, Santa Clara, CA).

Capillaries with total length of 48.5cm and effective length of 40cm were flushed daily for 10 minutes with a 1.0M NaOH solution. Between injections the capillary was flushed with acetone, nanopure water, and buffered nanodisc solution. Analytes were injected individually by 35 mBar of pressure for five seconds and detected at 210, 225, 245, and 254 nm. All analyses were run at 15 kv applied voltage and 25°C using 5 mM phospholipid concentration of nanodiscs in BGE.

The migration time and the effective electrophoretic mobility of the nanodiscs in the buffered solution was estimated by using the method of Bushey and Jorgenson[48, 49] using acetone as the EOF marker and the migration times of six alkyl-phenyl ketone homologs: acetophenone, propiophenone, butyrophenone, valerophenone, hexanophenone, and heptanophenone. The Excel application solver was used to determine the nanodisc migration time that gave the maximum r^2 for the plot of log retention factor vs homolog carbon number.

The retention factors for all analytes were calculated using the following equation,

$$k = \frac{\mu_{eo} - \mu_{\mathrm{sol}}}{\mu_{\mathrm{sol}} - (\mu_{eo} + \mu_{\mathrm{PSP}})}$$

where μeo is the electroosmotic flow during the analyte run determined by the migration time of acetone, μ_{sol} is the total (observed) electrophoretic mobility of the solute including the μ_{eo}, and μ_{PSP} is the electrophoretic mobility of the nanodiscs determined separately.

The logarithm of experimental $P_{o/w}$ and that of computationally derived $D_{pH7.0}$ were graphed against log of the respective retention factors for 38 probe solutes to determine the linear correlation. The log(DpH7.0) values were generated by ChemAxon software, which bases its computational methods on work by Viswanadhan et al[50] who generated values

through combination of atomic physiochemical properties. Linear Solvation Energy Relationships (LSER) characterization was performed using 32 LSER probe solutes similar to the list used in a recent study of a latex nanoparticle PSP[51]. After measurement of k values, Excel was used for multivariate linear regression to determine LSER coefficients.

3. Results and Discussion

3.1 Nanodisc characterization

The first reported use of copolymer belted nanodiscs was for solubilization of membrane bound proteins for spectroscopic studies[52]. Those nanodiscs were synthesized using a higher ratio of 3:1 (w:w) of belt to lipid[46]. For the purposes of EKC large ratios of copolymer belt to lipid were avoided in order to decrease the background UV absorbance. A lipid to belt ratio of 0.85:1 was used and yielded nanodiscs that were on average less than 20nm by Z-average diameter and intensity measurements (Table 1). For three of four syntheses, the measured diameters were not significantly different ($\alpha<0.05$) and averaged 17.8 nm, while a fourth synthesis yielded nanodiscs about 20% larger. According to the literature, decreasing the belt to lipid ratio may increase the size of the nanodisc[44]. The belt to lipid ratio used here was selected to provide nanodiscs of sufficiently small diameter to minimize light scattering while at the same time reducing background absorbance from the SMA polymer that would be observed at higher polymer to lipid ratios.

Separations of representative small molecule probes using the 0.85:1 nanodiscs as a PSP are presented in Figures 2 and 3. Figure 2 shows a separation of alkyl-substituted phenones with good plate counts and selectivity. These data were used to calculate a nanodisc electrophoretic mobility of $-3.44\times10^{-4}(cm^2/V*s)$. The reported electrophoretic mobility of SDS micelles is $-4.05\times10^{-4}(cm^2/V*s)$[49, 53], meaning that the nanodiscs have lower mobility and provide a narrower migration range than typical micellar PSPs. Still, the nanodisc electrophoretic mobility is sufficient to provide a useful migration range and allow measurable differences in migration time for solutes with differing affinity for the nanodiscs. The nanodisc generated an average of 230,000 theoretical plates for the compounds in Figure 2. The separation in Figure 3 also illustrates the good performance of the nanodisc PSP, providing good resolution, sufficient differences in migration time and an average of 180,000 theoretical plates. Both figures also show reproducible negative system peaks observed in this system. The belt polymers have significant absorbance at the wavelength of detection, and small changes in the background concentration of nanodiscs or styrene-containing impurities may be the cause of these system peaks.

3.2 Comparison of octanol-water partition coefficients to retention factors

Thirty-eight compounds with varying functional groups and size and with published values for $P_{o/w}$ [15, 54–57] (Table 2) were used to determine the effectiveness of these nanodiscs for indirect measurement of $P_{o/w}$ and $D_{pH7.0}$. Retention factors (k) for these were measured and are reported in Table 2. As detailed in the Supplemental Information, the volume ratio of lipid to BGE is approximately 0.003, meaning that equilibrium binding constants are about 300 times the retention factors. We have chosen not to convert our results to equilibrium constants prior to further analysis since the volume ratio is uncertain and the constant offset

to logarithm terms would not affect the outcomes. Correlations between log($P_{o/w}$) or log($D_{pH7.0}$) and log(k) were determined through linear regression.

The data for log($P_{o/w}$) are plotted in Figure 4, and it is clear that there are at least two different classes of solute probes with different relationships between log ($P_{o/w}$) and log (k). The primary difference between the two groups of solutes was found to be their hydrogen bond donor strength. The upper group of 22 solutes, with an r^2 value of 0.973 and a slope of 1.24±0.05, contains varying functionalities but none capable of donating a hydrogen bond. The second set of 16 solutes are hydrogen bond donors, and gave an r^2 value of 0.847 and a slope of 1.13±0.13. Regression of all 38 compounds gave an r^2 value of 0.881 and a slope of 1.31+/−0.08. There is not a single strong correlation for all solute chemistries, but good correlation and $P_{o/w}$ determination could be achieved within particular solute categories, especially depending on solute hydrogen bond donor strength. It is possible that solutes with more acidic hydroxyl groups versus those with more basic amine groups may have slightly different trends, but more solutes with amine functionalities would need to be analyzed to determine if a significantly different trend is present.

A plot of computationally derived log($D_{pH7.0}$) values vs log(k) is presented in Figure 5. Unlike Figure 4, there are no separate trends based on hydrogen bond strength. The r^2 value was 0.810 and the slope was 1.09±0.09. In general our retention factor results correlate better to experimental $P_{o/w}$ values than to computational $D_{pH7.0}$ values.

3.3 LSER analysis

In order to gain a better understanding of why the affinities of different classes of compounds correlate separately with $P_{o/w}$, linear solvation energy relationship (LSER) analysis was employed. LSER analysis is used to study the free energy for transfer of a solute from the BGE to the nanodisc. The free energy of transfer is modeled by the following equation,

$$\log(k) = c + vV + eE + sS + aA + bB$$

where the energy is treated as the sum of terms that include the McGowan characteristic volume (V), excess molar refraction (E), dipolarity/polarizability (S), hydrogen-bond acidity (A), and hydrogen-bond basicity (B) of the solute. The constant *c* accounts for the PSP to BGE volume ratio (phase ratio) and other factors not explained by the other descriptors. LSER uses experimental retention factors (k) and known solute descriptors (V,E,S,A,B) from a set of compounds to find the relative contribution of each solute property (coefficients *v,e,s,a,b*) via linear regression analysis. The solutes used for this LSER analysis and their descriptors are provided in Table 3. This model, proposed and developed by Abraham et al.[58], allows for the nanodiscs' solvation properties to be compared to other PSPs for which LSER was conducted with similar BGEs, octanol, and biological systems.

The LSER coefficients for the phospholipid nanodiscs are presented in Table 4, along with the LSER coefficients for synthetic vesicles[15], phospholipid vesicles[12], cationic surfactants[59], the octanol-water system, skin permeation studies and transmission across

the blood brain barrier. The skin permeation studies were completed using cadaver skin and stirred side by side in diffusion cells[60]. The blood brain barrier is the interface between the walls of the capillaries and the neural tissue[61]. Neither the skin permeation nor blood brain barrier measurements represent similar processes to the aqueous-nanodisc partitioning measurements reported here. They do provide an indication of how these values are affected by solute chemistry for comparison with the model solvent systems, including nanodisc EKC or octanol/water partitioning.

The *v* term is a measure of the increase in affinity of the PSP for solutes as the size of the solutes increases, and is a measure of the cohesiveness of the PSP relative to the BGE. The aqueous BGE in EKC is a relatively cohesive solvent, like water in octanol-water systems, and so the value for *v* in the EKC and octanol water systems is relatively large and positive. The relative magnitude of the values suggests that octanol is the least cohesive of the solvents or phases and that the nanodiscs are more cohesive and most similar to vesicles. No significant differences are observed between the nanodiscs, synthetic vesicles and phospholipid vesicles.

All of the PSPs and the octanol-water system have similar positive *e* terms, which represent the PSPs ability to interact with nonbonding and π electrons. The positive value for all systems indicates that they are more adept at interactions with nonbonding and π electrons than their aqueous counterparts. There are no statistically significant differences observed in the *e* values between different PSPs or octanol.

All of the systems shown have a negative *s* term signifying that more polar solutes are preferentially partitioned into the aqueous medium. The value for octanol is of significantly greater magnitude than for the EKC systems including the nanodiscs. This suggests that lipid bilayers and systems designed to model them are more polar than octanol, presumably because of the polar and ionic head groups. In this case, the model systems are more similar to the biological systems than is the octanol/water model.

The large negative *b* term for the nanodiscs, octanol and the other PSPs indicates that they are less able to interact with hydrogen bond acceptors (are less acidic) than their aqueous counterparts. The skin permeation *b* value is also negative and of similar magnitude, while the blood/brain barrier *b* term is a much smaller negative value indicating that it responds very differently to more basic solutes.

The *a* term is positive and of relatively large magnitude for the nanodiscs, and it is this term that shows the greatest difference between the nanodiscs and other model systems. A positive *a* term means that a PSP has a greater ability to accept a hydrogen bond (is more basic) than the BGE. This is consistent with the observation relative to $P_{o/w}$ above that hydrogen bond donor solutes behave differently as a class, with greater affinity for the nanodiscs than expected. The *a* terms for the octanol/water system and the phospholipid vesicles are not significantly different from 0, meaning solute acidity plays no measurable role in the solute partitioning in those systems. The nanodisc bilayer may be more able to accept hydrogen bonds because of the multiple carbonyls or the quaternary ammonium group located in the lipid head group, or the negative charge on the phosphate could allow

for electrostatic interactions with an acidic hydrogen. Norman et al.[62] showed that indole partitions favorably into the lipid bilayer near the hydrophobic core due to hydrogen bonding between indole's secondary amine and lipid carbonyl groups. The cationic surfactant micelles also have positive values for *a* of about unit magnitude, which is reported for all cationic micelles.[59] This suggests that the positive *a* value for these nanodiscs is related to the presence of a quaternary amine in the head group. It should be noted that the *a* value for the nanodiscs could result from interactions with carbonyl groups on the copolymer belt, although a large positive *a* term is not typically associated with acrylate-containing polymeric PSPs[6, 63]. Our preliminary experiments indicate weak or no interaction between probe solutes and the polymer alone as a PSP (data not shown). Future experiments will probe this in greater detail as well as investigate and confirm the effect of lipid head group chemistry on the solvation environment.

4. Conclusions

Phospholipid bilayer nanodiscs with synthetic polymer belts have been introduced as a PSP in EKC and demonstrated good performance. The use of a synthetic polymer in place of belt proteins allows the nanodiscs to be generated affordably and in sufficient quantity for use in EKC. The nanodiscs have sufficient electrophoretic mobility to allow for a good migration range and generate high theoretical plate counts. Together, this results in high peak capacity and excellent ability to separate, resolve and distinguish analytes of similar chemistry and structure.

More significantly, the nanodiscs offer a representative model of biological phospholipid bilayers that can be dispersed in BGE and studied by EKC. By this approach, the affinity of the bilayer structure for probe solutes can be determined and characterized.

One application of this method could be to calibrate retention vs $P_{o/w}$ in order to estimate or determine $P_{o/w}$ values quickly and inexpensively. Nanodisc retention factors for particular classes of compounds have been shown to correlate well with $P_{o/w}$, suggesting that this is a viable approach. However, it is clear that, due to specific localized interactions with the phospholipid used in this study, the method could not be applied generally and would require calibration with standards of similar chemistry to the compound of interest. Alternatively, other lipid structures incorporated into nanodiscs might provide better and more general correlation of retention with $P_{o/w}$.

A potentially significant application of this technology relative to other PSPs could be to measure and characterize interactions between solutes and lipid bilayers directly. Nanodiscs with lipid composition similar to specific biological membranes could be generated and studied. LSER analysis of the nanodisc-solute interactions in this study demonstrates that the nanodiscs provide a solvation environment with low cohesivity and weak hydrogen bond donating ability, similar in many respects to micelles, vesicles and octanol. However, the nanodiscs also provide relatively strong hydrogen bond acceptor strength, similar to cationic micelles but significantly different from vesicles and octanol. This affinity for hydrogen bond donors is likely due to interactions with the phosphocholine head group, demonstrating

that the approach is sensitive to specific localized interactions with the phospholipids and should be sensitive to changes in lipid composition.

Supplementary Material

Refer to Web version on PubMed Central for supplementary material.

References

1. Terabe S, Otsuka K, Ichikawa A, Tsuchiya A, Ando T. Anal Chem. 1984; 56:111–113.
2. Palmer CP. Scientia Chromatographica. 2015; 7:1–23.
3. Pyell, U., editor. Electrokinetic Chromatography Theory, Instrumentation and Applications. John Wiley and Sons Ltd; West Sussex, England: 2006.
4. Altria KD. J Chromatogr A. 2000; 892:171–186. [PubMed: 11045487]
5. Yang H, Ding Y, Cao J, Li P. Electrophoresis. 2013; 34:1273–1294. [PubMed: 23463608]
6. Palmer CP. Electrophoresis. 2002; 23:3993–4004. [PubMed: 12481289]
7. Palmer, CP. Electrokinetic Chromatography Theory, Instrumentation and Applications. Pyell, U., editor. John Wiley and Sons Ltd; West Sussex, England: 2006.
8. Palmer CP. Electrophoresis. 2009; 30:163–168. [PubMed: 19107699]
9. Nilsson C, Viberg P, Spégel P, Jömtén-Karlsson M, Petersson P, Nilsson S. Anal Chem. 2006; 78:6088–6095. [PubMed: 16944888]
10. Palmer CP, Hilder EF, Quirino JP, Haddad PR. Anal Chem. 2010; 82:4046–4054. [PubMed: 20402470]
11. Wiedmer SK, Holopainen JM, Mustakangas P, Kinnunen PKJ, Riekkola ML. Electrophoresis. 2000; 21:3191–3198. [PubMed: 11001217]
12. Pascoe RJ, Foley JP. Electrophoresis. 2003; 24:4227–4240. [PubMed: 14679570]
13. Hong M, Weekley B, Grieb SJ, Foley JP. Anal Chem. 1998; 70:1394–1403. [PubMed: 21644734]
14. Poole SK, Poole CF. J Chromatogr B. 2003; 797:3–19.
15. Klotz WL, Schure MR, Foley JP. J Chromatogr A. 2002; 962:207–219. [PubMed: 12198964]
16. Burns ST, Agbodjan AA, Khaledi MG. J Chromatogr A. 2002; 973:167–176. [PubMed: 12437175]
17. Burns ST, Khaledi MG. J Pharm Sci. 2002; 91:1601–1612. [PubMed: 12115822]
18. Carrozzino JM, Khaledi MG. Pharm Res. 2004; 21:2327–2335. [PubMed: 15648265]
19. Ruokonen SK, Duša F, Lokajová J, Kilpeläinen I, King AWT, Wiedmer SK. J Chromatogr A. 2015; 1405:178–187. [PubMed: 26072299]
20. Wiedmer SK, Kulovesi P, Riekkola ML. J Sep Sci. 2008; 31:2714–2721. [PubMed: 18693313]
21. Wiedmer SK, Lokajová J. J Sep Sci. 2013; 36:37–51. [PubMed: 23213065]
22. Wang Y, Sun J, Liu H, Liu J, Zhang L, Liu K, He Z. Analyst. 2009; 134:267–272. [PubMed: 19173048]
23. Xian DL, Huang KL, Liu SQ, Xiao JY. Chin J Chem. 2008; 26:671–676.
24. Wang Y, Sun J, Liu H, He Z. Electrophoresis. 2007; 28:2391–2395. [PubMed: 17578839]
25. Xian D, Huang K, Liu S, Xiao J. Chromatographia. 2008; 67:407–412.
26. Wang T, Feng Y, Jin X, Fan X, Crommen J, Jiang Z. J Pharm Biomed Anal. 2014; 96:263–271. [PubMed: 24814828]
27. Ishihama Y, Oda Y, Asakawa N. Anal Chem. 1996; 68:1028–1032.
28. Ishihama Y, Oda Y, Asakawa N. Anal Chem. 1996; 68:4281–4284. [PubMed: 21619339]
29. Ishihama Y, Oda Y, Uchikawa K, Asakawa N. Anal Chem. 1995; 67:1588–1595.
30. Henchoz Y, Romand S, Schappler J, Rudaz S, Veuthey JL, Carrupt PA. Electrophoresis. 2010; 31:952–964. [PubMed: 20191557]
31. Jia Z, Mei L, Lin F, Huang S, Killion RB. J Chromatogr A. 2003; 1007:203–208. [PubMed: 12924566]

32. Klotz WL, Schure MR, Foley JP. J Chromatogr A. 2001; 930:145–154. [PubMed: 11681572]
33. Øtergaard J, Honore Hansen Steen S, Larsen C, Schou C, Heegaard NHH. Electrophoresis. 2003; 24:1038–1046. [PubMed: 12658693]
34. Poole SK, Durham D, Kibbey C. J Chromatogr B. 2000; 745:117–126.
35. Poole SK, Patel S, Dehring K, Workman H, Dong J. J Chromatogr B. 2003; 793:265–274.
36. Tu J, Halsall HB, Seliskar CJ, Limbach PA, Arias F, Wehmeyer KR, Heineman WR. J Pharm Biomed Anal. 2005; 38:1–7. [PubMed: 15907611]
37. Xia Z, Jiang X, Mu X, Chen H. Electrophoresis. 2008; 29:835–842. [PubMed: 18203250]
38. Xia Z, Yang J, Li L, Yang F, Jiang X. Chromatographia. 2010; 72:495–501.
39. Wan H, Åhman M, Holmén AG. J Med Chem. 2009; 52:1693–1700. [PubMed: 19256501]
40. Bayburt TH, Sligar SG. FEBS Letters. 2010; 584:1721–1727. [PubMed: 19836392]
41. Denisov IG, Sligar SG. Nat Struct Mol Biol. 2016; 23:481–486. [PubMed: 27273631]
42. Hernandez-Rocamora VM, Garcia-Montanes C, Rivas G. Curr Top Med Chem. 2014; 14:2637–2646. [PubMed: 25515754]
43. Ritchie, TK., Grinkova, YV., Bayburt, TH., Denisov, IG., Zolnerciks, JK., Atkins, WM., Sligar, SG. Meth Enzymol. Nejat, D., editor. Academic Press; 2009. p. 211-231.
44. Dörr JM, Scheidelaar S, Koorengevel MC, Dominguez JJ, Schäfer M, van Walree CA, Killian JA. Eur Biophys J. 2016; 45:3–21. [PubMed: 26639665]
45. Jamshad M, Grimard V, Idini I, Knowles TJ, Dowle MR, Schofield N, Sridhar P, Lin Y, Finka R, Wheatley M, Thomas ORT, Palmer RE, Overduin M, Govaerts C, Ruysschaert JM, Edler KJ, Dafforn TR. Nano Res. 2015; 8:774–789.
46. Scheidelaar S, Koorengevel MC, Pardo JD, Meeldijk JD, Breukink E, Killian JA. Biophys J. 2015; 108:279–290. [PubMed: 25606677]
47. Swainsbury DJK, Scheidelaar S, van Grondelle R, Killian JA, Jones MR. Angew Chem, Int Ed. 2014; 53:11803–11807.
48. Bushey MM, Jorgenson JW. Anal Chem. 1989; 61:491–493.
49. Bushey MM, Jorgenson JW. J Microcol Sep. 1989; 1:125–130.
50. Viswanadhan VN, Ghose AK, Revankar GR, Robins RK. J Chem Inform Comp Sci. 1989; 29:163–172.
51. Hyslop JS, Hall LMG, Umansky AA, Palmer CP. Electrophoresis. 2014; 35:728–735. [PubMed: 24302072]
52. Knowles TJ, Finka R, Smith C, Lin YP, Dafforn T, Overduin M. J Am Chem Soc. 2009; 131:7484–7485. [PubMed: 19449872]
53. Schulte S, Palmer CP. Electrophoresis. 2003; 24:978–983. [PubMed: 12658685]
54. Cabot JM, Subirats X, Fuguet E, Roses M. ADMET and DMPK. 2014; 2:98–106.
55. Ellington, JJ., Floyd, TF. US EnvironmentalProtection Agency. Athens, GA: 1996.
56. Leo A, Hansch C, Elkins D. Chem Rev+. 1971; 71:525–616.
57. Sangster J. J Phys Chem Ref Data. 1989; 18:1111–1229.
58. Abraham MH, Chadha HS, Martins F, Mitchell RC, Bradbury MW, Gratton JA. Pesticide Science. 1999; 55:78–88.
59. Schnee VP, Palmer CP. Electrophoresis. 2008; 29:777–782. [PubMed: 18297645]
60. Johnson ME, Blankschtein D, Langer R. J of Pharm Sci. 1995; 84:1144–1146. [PubMed: 8537898]
61. Abbott NJ, Patabendige AAK, Dolman DEM, Yusof SR, Begley DJ. Neurobiol Dis. 2010; 37:13–25. [PubMed: 19664713]
62. Norman KE, Nymeyer H. Biophys J. 2006; 91:2046–2054. [PubMed: 16815896]
63. Yang S, Bumgarner JG, Khaledi MG. J Chromatogr A. 1996; 738:265–274. [PubMed: 8696506]
64. Schnee VP, Palmer CP. Electrophoresis. 2008; 29:767–776. [PubMed: 18297644]

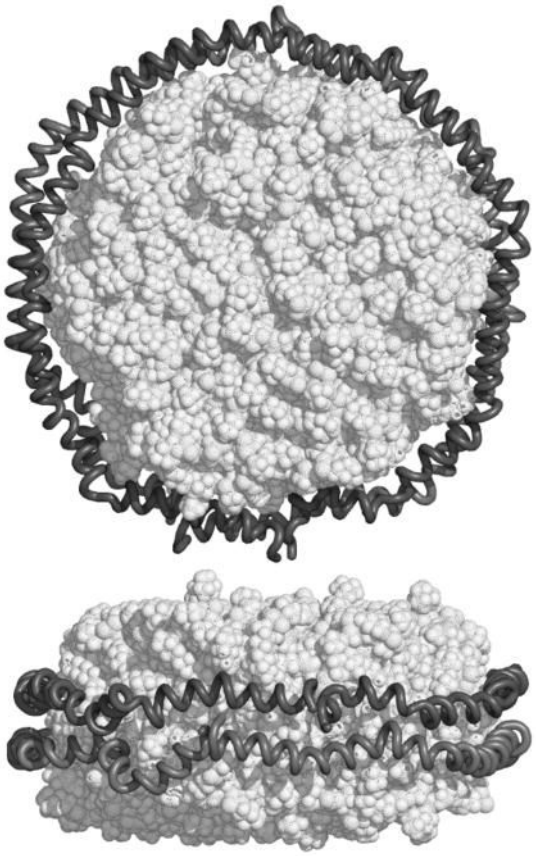

Fig. 1.
Structure of a nanodisc with protein belts. Reproduced from [43] with permission of the authors.

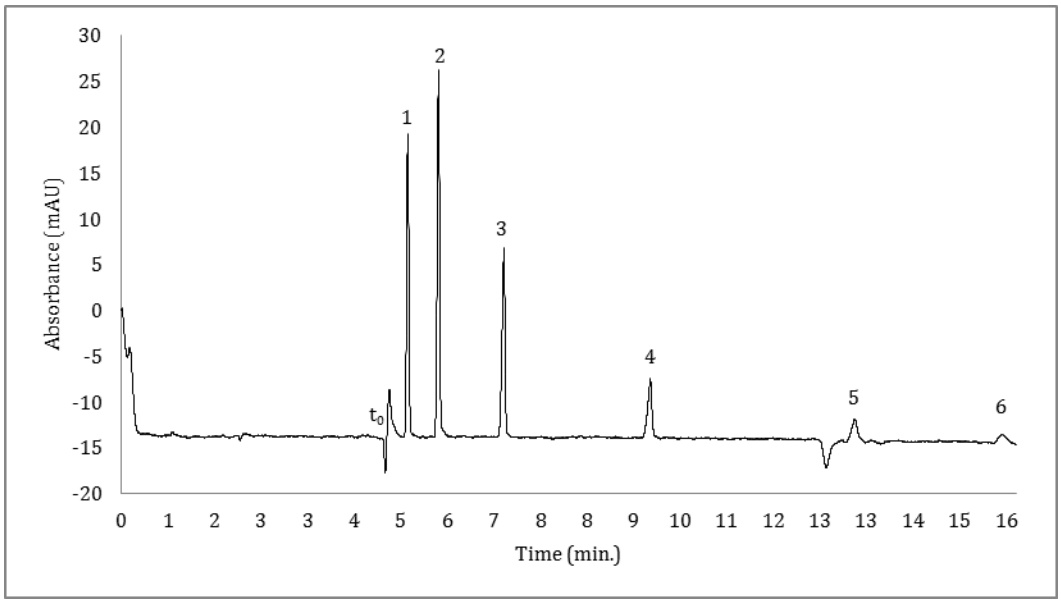

Fig. 2.

Separation of six alkyl-phenone solutes: (1) Acetophenone, (2) Propiophenone, (3) Butyrophenone, (4) Valerophenone, (5) Hexanophenone, and (6) Heptanophenone. Separation parameters: 5 mM phospholipid nanodisc with 1:0.85 (w:w) lipid to belt ratio, in a 25 mM phosphate pH 7.0. Capillary dimensions: 48.5 cm × 50μm I.D. with a 150μm extended cell pathlength. The injection was made with 35 mbar of pressure for 5 seconds. The operating voltage was 15 kV with detection at 245 nm. The negative peaks shown in the electropherogram are system peaks.

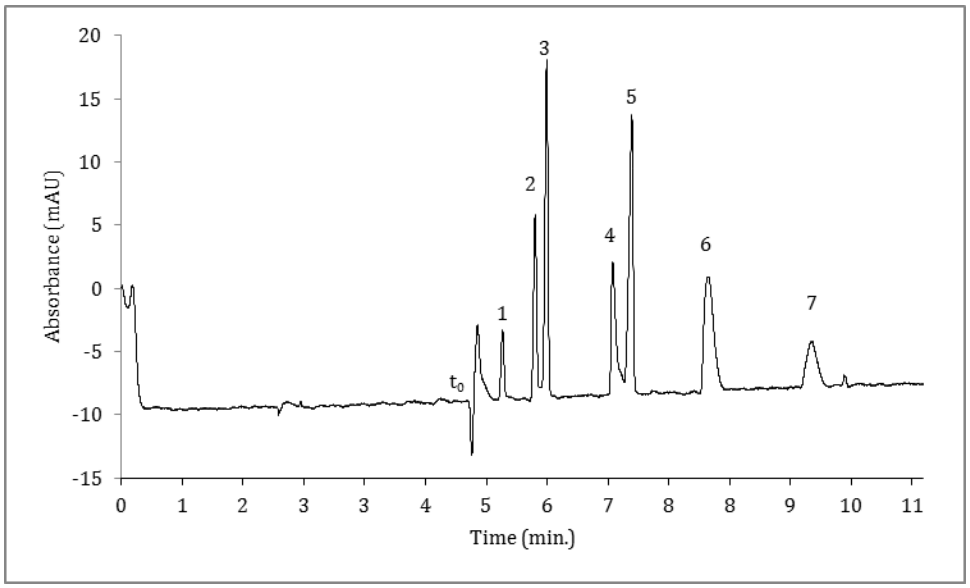

Fig. 3.

Separation of solutes: (1) Benzonitrile, (2) Nitrobenzene, (3) Methyl Benzoate, (4) 4-Nitroaniline, (5) Ethyl Benzoate, (6) Indole, and (7) 4-Chlorophenol. The analysis conditions were the same as in Fig. 1, with detection at 245 nm.

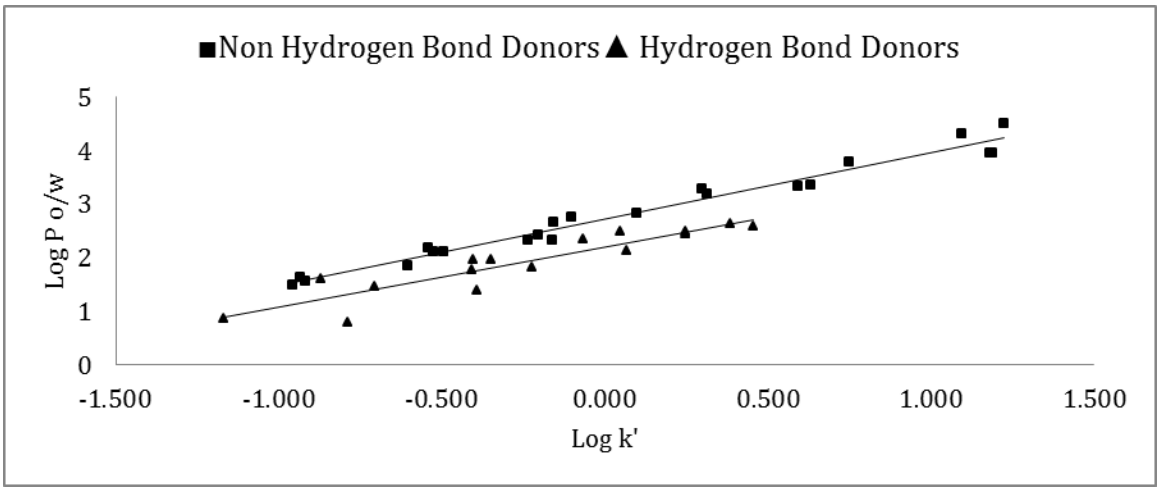

Fig. 4.
Plot of log $P_{o/w}$ versus log k for nanodisc system.

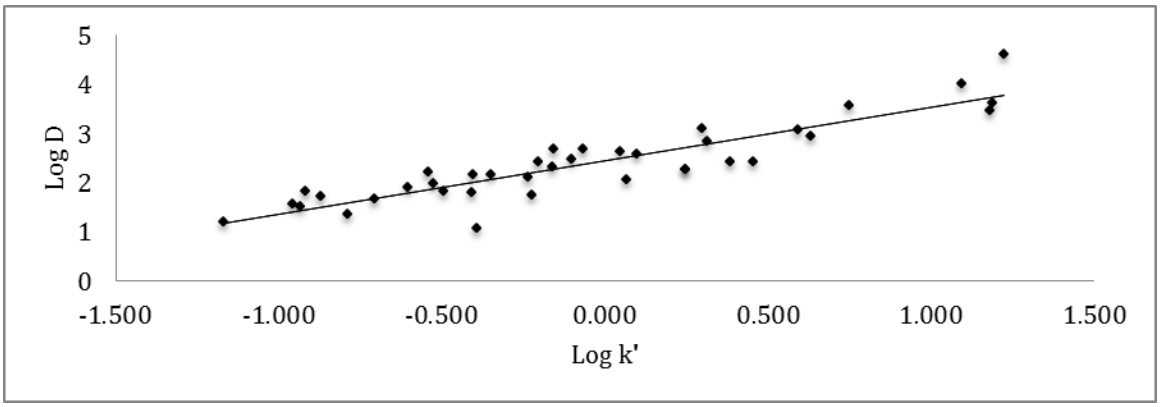

Fig. 5.
Plot of computationally derived log(DpH7.0) values vs log(k).

Table 1

Characteristics of nanodiscs of different composition.

Sample 1	Z-Average (d.nm)	Intensity (d.nm)
Trial 1	21.6±6.0	23.0±10.3
Trial 2	21.7±6.0	23.8±10.8
Trial 3	21.6±5.4	24.4±11.4
Sample 2		
Trial 1	17.9±6.3	17.2±7.0
Trial 2	17.9±5.5	17.6±7.0
Trial 3	17.8±5.8	18.2±8.0
Sample 3		
Trial 1	18.0±5.9	16.8±6.2
Trial 2	17.7±5.3	18.7±8.6
Trial 3	17.7±5.0	18.6±8.2
Sample 4		
Trial 1	17.6±5.7	16.7±6.3
Trial 2	17.7±5.3	17.6±7.0
Trial 3	17.9±5.4	19.3±9.5

Table 2

Probe solutes and their $P_{o/w}$ values [15, 54–57]

Compound List	Log $P_{o/w}$ Values	Log D Values	k value	Compound List	Log $P_{o/w}$ Values	Log D Values	k Value
Resorcinol	0.80	1.36	0.163±0.001	3,5-Dimethylphenol	2.35	2.70	0.858±0.002
Benzyl Alcohol	0.87	1.21	0.068±0.0001	4-Nitrotoluene	2.42	2.43	0.627±0.007
4-Nitroaniline	1.39	1.08	0.405±0.099	4-Chlorophenol	2.44	2.27	1.77±0.04
Phenol	1.46	1.67	0.197±0.0005	3-Chlorophenol	2.50	2.27	1.76±0.01
Phenyl Acetate	1.49	1.58	0.111±0.0007[4]	4-Ethylphenol	2.50	2.63	1.12±0.03
Benzonitrile	1.56	1.83	0.121±0.0004	4-Bromophenol	2.59	2.43	2.86±0.015
3-Methyl Benzyl Alcohol	1.60	1.72	0.135±0.0009	3-Bromophenol	2.63	2.43	2.42±0.008
Acetophenone	1.63	1.53	0.116±0.0009	Butyrophenone	2.66	2.68	0.700±0.0009
4-Fluorophenol	1.77	1.81	0.390±0.002	Methyl-o-Toluate	2.75	2.49	0.789±0.003
4-Chloroaniline	1.83	1.75	0.559±0.0006	Chlorobenzene	2.84	2.58	1.25±0.01
Nitrobenzene	1.86	1.91	0.248±0.0004	Propylbenzoate	3.18	2.86	2.06±0.01
m-Cresol	1.96	2.18	0.396±0.004	Valerophenone	3.28	3.12	1.99±0.02
p-Cresol	1.97	2.18	0.448±0.001	4-Chlorotoluene	3.33	3.09	3.92±0.06
Anisole	2.11	1.82	0.321±0.001	Naphthalene	3.37	2.96	4.33±0.25
Methyl Benzoate	2.12	1.98	0.297±0.003	Hexanophenone	3.79	3.57	5.62±0.53
Indole	2.14	2.07	1.17±0.017	1-Methyl Naphthalene	3.95	3.48	15.4±3.4
Propiophenone	2.19	2.23	0.287±0.0006	Biphenyl	3.95	3.62	15.6±2.7
4-Chloroacetophenone	2.32	2.13	0.584±0.0009	Heptanophenone	4.32	4.01	12.5±0.7
Ethylbenzoate	2.33	2.33	0.692±0.005	Dibutyl Phathalate	4.50	4.63	16.8±0.5

Table 3

LSER Solutes and their solvation parameters[51]

Solute[22]	v	e	s	α	β	Solute[22]	v	e	s	α	β
1-Methyl Naphthalene	1.226	1.344	0.900	0.000	0.200	Benzonitrile	0.871	0.742	1.110	0.000	0.330
3-Bromophenol	0.950	1.060	1.150	0.700	0.160	Benzyl Alcohol	0.923	0.832	0.870	0.370	0.560
3-Chlorophenol	0.898	0.909	1.060	0.690	0.150	Biphenyl	1.324	1.360	0.990	0.000	0.220
3-Methyl Benzyl Alcohol	1.057	0.815	0.900	0.330	0.590	Chlorobenzene	0.839	0.718	0.650	0.000	0.070
3,5-Dimethylphenol	1.057	0.820	0.840	0.570	0.360	Ethylbenzoate	1.214	0.689	0.850	0.000	0.460
4-Bromophenol	0.950	1.080	1.170	0.670	0.200	Indole	0.946	1.200	1.120	0.440	0.220
4-Chloroacetophenone	1.136	0.955	1.090	0.000	0.440	m-Cresol	0.916	0.822	0.880	0.570	0.340
4-Chloroaniline	0.939	1.060	1.130	0.300	0.310	Methyl Benzoate	1.073	0.733	0.850	0.000	0.460
4-Chlorophenol	0.898	0.915	1.080	0.670	0.200	Methyl-o-Toluate	1.214	0.772	0.870	0.000	0.430
4-Chlorotoluene	0.980	0.705	0.670	0.000	0.070	Naphthalene	1.085	1.340	0.920	0.000	0.200
4-Ethylphenol	1.057	0.800	0.900	0.550	0.360	Nitrobenzene	0.891	0.871	1.110	0.000	0.280
4-Fluorophenol	0.793	0.670	0.970	0.630	0.230	p-Cresol	0.916	0.820	0.870	0.570	0.310
4-Nitroaniline	0.990	1.220	1.910	0.420	0.380	Phenol	0.775	0.805	0.890	0.600	0.300
4-Nitrotoluene	1.032	0.870	1.110	0.000	0.280	Phenyl Acetate	1.073	0.661	1.130	0.000	0.540
Acetophenone	1.014	0.818	1.010	0.000	0.480	Propiophenone	1.155	0.804	0.950	0.000	0.510
Anisole	0.916	0.708	0.750	0.000	0.290	Resorcinol	0.834	0.980	1.000	1.100	0.580

Table 4

LSER parameter results

	Nanodiscs	O/W[58][a]	CTAB-SOS[15]	POPC/PS[12]	C_{16}TMAB[64]	Blood/Brain Barrier Rats[58][a]	Skin Permation Studies[58][a]
v	3.04 (0.10)	3.81 (0.12)	2.85 (0.16)	2.68 (0.25)	3.28 (0.22)	1.00 (0.20)	2.01 (0.20)
e	0.60 (0.07)	0.56 (0.12)	0.56 (0.13)	0.70 (0.22)	0.65 (0.13)	0.20 (0.20)	0.44 (0.20)
s	−0.36 (0.05)	−1.05 (0.12)	−0.57 (0.12)	−0.54 (0.18)	−0.58 (0.11)	−0.69 (0.20)	−0.41 (0.20)
a	0.57 (0.04)	0.03 (0.12)	0.23 (0.09)	0.02 (0.17)	1.06 (0.09)	−0.72 (0.20)	−1.63 (0.20)
b	−3.26 (0.08)	−3.46 (0.12)	−3.25 (0.18)	−2.90 (0.30)	−2.77 (0.18)	−0.70 (0.20)	−3.29 (0.20)

[a] values in parenthesis are reported as standard deviation and not standard error